
Effects of Variable Viscosity on Unsteady Natural Convection Hydromagnetic Flow Past an Isothermal Sphere

Mwangi Wanjiku Lucy^{1,2}, Mathew Ngugi Kinyanjui¹, Roy Phineas Kiogora¹

¹Department of Pure and Applied Mathematics, Jomo Kenyatta University of Agriculture and Technology, Nairobi, Kenya

²Pan African University, Institute for Basic Sciences, Technology and Innovation, Nairobi, Kenya

Email address:

Lcywanjiku@gmail.com (M. W. Lucy)

To cite this article:

Mwangi Wanjiku Lucy, Mathew Ngugi Kinyanjui, Roy Phineas Kiogora. Effects of Variable Viscosity on Unsteady Natural Convection Hydromagnetic Flow Past an Isothermal Sphere. *American Journal of Applied Mathematics*. Vol. 4, No. 6, 2016, pp. 258-270.

doi: 10.11648/j.ajam.20160406.11

Received: September 13, 2016; **Accepted:** October 2, 2016; **Published:** November 1, 2016

Abstract: In this study, the effects of variable viscosity on unsteady natural convection hydromagnetic flow past an isothermal sphere are determined. The uniformly heated sphere is immersed in a viscous and incompressible fluid where viscosity of the fluid is taken as a linear function of temperature. The Partial Differential Equations governing the flow are reduced into non dimensional form and since these equations are non-linear, they are solved numerically using finite difference methods. The numerical results obtained are presented graphically and discussed. It has been observed that there is a significant change in primary velocity, secondary velocity, temperature, skin friction and heat transfer of the fluid with changes in Reynolds number, Grashof number, Magnetic parameter and viscous variation parameter. These results are applicable in engineering, technology and biomedical fields.

Keywords: Natural Convection, Hydrodynamics, Temperature Dependence of Liquid Viscosity, Isothermal Sphere, Finite Difference, Dimensional Analysis

1. Introduction

Fluid is a substance that is capable of flowing. It can also be defined as a substance which deforms continuously when subjected to external shearing stress. Fluids are classified as Liquid, Gas, Vapor, Ideal Fluids and Real Fluids. A liquid is fluid which possesses a definite volume which varies slightly with temperature and pressure. A gas possesses no definite volume and is compressible. Vapor is a gas whose temperature is such that it is very near the liquid state. In liquids, molecules are close together compared to the molecules in gases which are not close to one another and are in a haphazard movement in all directions which make them to collide with each other. Ideal fluid is one which is compressible and has no viscosity and surface tension whereas a real fluid is one which has viscosity, surface tension and compressibility in addition to density. In real world, ideal fluids do not exist but real fluids exist.

Fluid flow can be classified as steady and unsteady

depending on their variation with time. A steady flow is one in which the fluid characteristics like velocity, pressure and density change with time whereas unsteady flow is one in which the velocity, pressure or density at a point change with respect to time. Other types of fluid flows include Uniform, Non Uniform, Rotational, Irrotational, Laminar, Turbulent, Compressible and incompressible flows.

The study of electric conducting fluids has gained popularity in our world today. These fluids include plasmas, liquid metals, salt water and air. This has attracted many researchers to carry out research in the same field. This is because it has found its application in many areas since it involves study of electrically conducting fluids. These fluids can be found in areas such as the production of electricity power especially in electrical plants and in the geothermal plants in Kenya. The interaction of the current with the magnetic field changes the motion of the fluid and produces an induced magnetic field.

An isothermal sphere in this study is a uniformly heated

perfect geometrical object that is made of non-conducting material. Natural convection flow from an isothermal horizontal cylinder was investigated by Molla *et al* (2005) where viscosity was taken as an inverse function of temperature. This study was observed to be appropriate for fluids having large Prandtl number. The researchers observed that there was an increase in the rate of heat transfer and a decrease in the rate of skin-friction coefficient due to the effect of Rayleigh number Ra and viscosity variation parameter. It was also observed that the momentum and thermal boundary layer become thinner where there is an increase in the values of viscosity-variation parameter. Both viscosity and velocity distribution was observed to increase whereas the temperature distributions were observed to decrease with the effect of Rayleigh number Ra and there was an enhancement of the thickness of momentum boundary layer.

Umavathi, (2015) studied the combined effect of variable viscosity and thermal conductivity of a viscous fluid on free convection flow in a vertical channel using DTM. It was found out that increasing the viscosity led to enhancement of the flow and heat transfer. Also, increasing the variable thermal conductivity led to suppression of the flow and the heat transfer for variable viscosity. Therefore, unsteady natural hydrodynamic convection flow is a phenomenon that is of great importance in our world today.

Unsteady magnetohydrodynamic heat transfer with thermal radiation flux in a semi-infinite porous medium was investigated by B'eg *et al* (2011). In this case, they considered analytical and numerical study. They observed that an increase in Hartmann number through a strong magnetic flux density causes a decrease in the flow velocity, u with distance normal to the plate surface into the boundary layer. This shows that changes in Hartmann number cause a significant change in the velocity. Their results showed that thermal radiation increase fluid temperatures and accelerates the flow whereas magnetic field simulated by the Hartmann number decelerates the flow and reduces the shear stress. They also observed that through the assistance of buoyancy forces, Darcian drag impedes the flow and increasing free convection accelerates the flow. It was concluded that increase in Prandtl number decreases temperature whereas the velocity gradient increases.

Unsteady natural convection flow past a vertical accelerated plate has been investigated by Deka *et al* (2009) where the plate was placed in a thermally stratified fluid. In their study, they used the Laplace transform techniques to solve the equations that they obtained. They observed that thermal stratification parameter S is an important factor in the study of unsteady vertical natural convection flow. This is due to the fact that velocity in thermally stratified fluid decreases with the increase of stratification parameter S and increases when Gr and t increase. They also observed that there is a decrease in temperature with increase in the value of Grashof number and Stratification parameter S . It was observed that Skin Friction, Nusselt number increases with increase in the values of S . Mina *et al* (2004) investigated

similarity solutions for unsteady free-convection from a continuous moving vertical surface. These researchers used the shooting method to solve the obtained differential equations in order to obtain analytical solution for temperature and numerically for velocity. Their results showed that increase in Prandtl number (Pr) leads to decrease in the thickness of the thermal boundary-layer and also a decrease in the vertical velocity (u).

The unsteady free convection flow with thermal radiation past a porous vertical plate with Newtonian heating was studied by Mebine *et al* (2009). They used the technique of Laplace transform in deriving the solutions to the governing flow and energy equations. It was concluded that increase in suction, radiation parameter, blowing and free convection parameter leads to increase in the velocity where it reaches to a maximum point and then starts to decrease up to zero at the edge of the boundary layer. They also observed that there is a decrease in temperature as radiation parameter and suction increases whereas increase in blowing retards the flux of heat to the flow and there is an increase in temperature due to increase in suction.

Ramesh *et al* (2011) investigated unsteady flow of a conducting dusty fluid between two circular cylinders. The variable separable method was used in their study in order to obtain the solutions. In their results, they observed that the graphs of velocity profiles are parabolic in nature for different values of Hartmann number and Time (T). Another observation by these researchers is that magnetic field retards the flow of both the fluid and dust phases as shown by the effects of Hartmann number and time increase leads to decrease in velocity. When the dust particles are very fine, then the velocities for both fluid and dust are the same.

Effect of inclined magnetic field on unsteady free convection flow of a dusty and viscous fluid between two infinite flat plates filled by a porous medium was investigated by Sugunamma *et al* (2013). They used the perturbative technique to solve the governing equations. In their results, they observed that when $Gr > 0$, velocity decreases with increase of magnetic parameter and also when (Porous parameter) increases. It was observed that there is gradual decrease of velocity with increase in time and (Heat source parameter). It was also observed that increase in Gr causes gradual increase in fluid velocity and particle velocity and that as Pr increases, the velocity of both the fluid and the particle phase decreases. The researchers also found out that an increase in ϕ (Volume fraction of dusty particles) causes an increase in fluid velocity and particle velocity and that there is a decrease in temperature of the dusty fluid when there is an increase in time.

Mutua, (2013) investigated the magnetohydrodynamic free convection flow of a heat generating fluid past a semi-infinite vertical porous plate. In this case, they considered the plate with variable suction. They used the finite difference method and observed that decrease in rotational parameter leads to increase in the velocity profiles. It was also observed that there was an increase in the velocity profiles when Eckert number and Magnetic parameter increase and on

removal of injection. There was no effect observed on the primary velocity profile when Suction parameter was increased but there was a decrease in the secondary velocity profile.

Seethamahalakshmi, (2012) studied the MHD free convective mass transfer flow past an infinite vertical porous plate with variable suction. They also considered the study with solet effects. In their study, they observed that increase in Prandtl number leads to decrease in velocity and increase in Soret number also leads to increase in the velocity field. Also decrease in the applied magnetic intensity contributes to a decrease in velocity whereas a decrease in temperature was observed when Prandtl number increases.

Recently, Deepa *et al* (2014) investigated the effects of viscous dissipation on unsteady MHD free convective flow. They considered the convective flow with thermophoresis past a radiate, inclined and permeable plate. The implicit finite difference scheme with shooting method was used to solve the obtained governing equations. They found out that there is an increase in the viscous drag as well as the rate of heat transfer when there is a significant variation of viscosity. They made a conclusion that there is an induced concentration of the particles for a destructive reaction and reduction of generative reaction when there is higher order of chemical reaction.

From the research work cited above, it can be seen that extensive research work has been carried out on MHD natural convection fluid flow past a surface. However, no emphasis has been given to the problem studied by Molla *et al* (2012) considering unsteady flow where viscosity as a linear function of temperature. Therefore, this work presents findings of studies on the effects of variable viscosity on unsteady natural convection hydromagnetic flow past an isothermal sphere taking viscosity as linear function of temperature and analysis of the results using Direct Numerical Scheme.

2. Formulation

The configuration of the problem considered in this study is as shown in the diagram below;

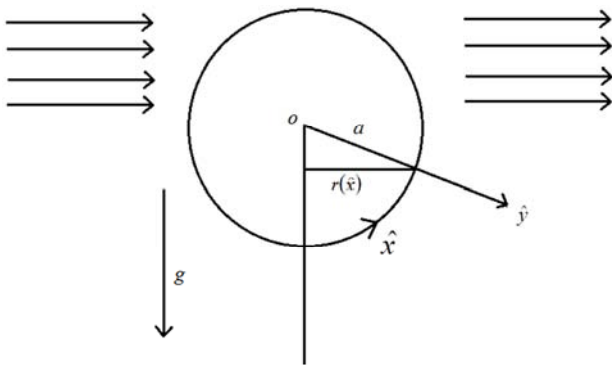


Figure 1. Physical Model of the Problem.

The diagram above shows a two-dimensional Laminar free convective hydromagnetic fluid flow past a uniformly heated

sphere Centre (o) and radius (a) which is immersed in a viscous and incompressible fluid. Viscosity of the fluid is taken as a linear function of temperature, thus, viscosity varies directly proportional to temperature

2.1. Governing Equations

2.1.1. Equation of Conservation of Mass

This equation states that mass can neither be created nor destroyed under normal conditions. It is obtained from the fact that mass fluid entering and leaving a volume in the flow field have the same mass balance.

$$\frac{\partial \rho}{\partial t} + \vec{\nabla} \cdot (\rho \vec{q}) = 0 \tag{1}$$

Where \vec{q} is the velocity in the X, Y and Z direction and

$$\vec{\nabla} = \hat{i} \frac{\partial}{\partial \hat{x}} + \hat{j} \frac{\partial}{\partial \hat{y}} + \hat{k} \frac{\partial}{\partial \hat{z}} \tag{2}$$

2.1.2. Equation of Motion

The expression of the equation in vector form is given as;

$$\frac{\partial \vec{q}}{\partial t} + \vec{q} (\vec{\nabla} \cdot \vec{q}) = -\frac{1}{\rho} \vec{\nabla} p + \nu \nabla^2 \vec{q} + \vec{F} \tag{3}$$

Where $\frac{\partial \vec{q}}{\partial t}$ is the temporal acceleration, $\vec{q} (\vec{\nabla} \cdot \vec{q})$ is the convective acceleration, $\vec{\nabla} p$ is the pressure gradient, $\nu \nabla^2 \vec{q}$ is the force due to viscosity and \vec{F} represents the body forces vector in X and Y directions.

2.1.3. The Energy Equation

The general equation is given as:

$$\rho C_p \left(\hat{u} \frac{\partial T}{\partial \hat{x}} + \hat{v} \frac{\partial T}{\partial \hat{y}} \right) = K \left(\frac{\partial^2 T}{\partial \hat{x}^2} + \frac{\partial^2 T}{\partial \hat{y}^2} \right) + \mu \phi \tag{4}$$

Where viscous energy dissipation term ϕ is defined as:

$$\phi = 2 \left[\left(\frac{\partial u}{\partial x} \right)^2 + \left(\frac{\partial v}{\partial y} \right)^2 \right] + \left(\frac{\partial u}{\partial y} + \frac{\partial v}{\partial x} \right)^2 \tag{5}$$

2.2. Non-dimensional Parameters

In this study, the following non-dimensional numbers will be encountered while taking the analysis of various equations:

2.2.1. Prandtl Number, Pr

This number gives the ratio of viscous force to the thermal and is defined as:

$$Pr = \frac{\mu C_p}{K}$$

2.2.2. Grashof Number, Gr

This number gives the relative importance of buoyancy

force to viscous force. This number usually occurs in natural convection problem and is usually defined as:

$$Gr = \frac{g\beta(T_w - T_\infty)a^3}{V_\infty^2}$$

2.2.3. Magnetic Parameter, M

This is defined as;

$$M = \frac{\delta_0\beta_0^2 a^2}{\mu_\infty Gr^{\frac{1}{2}}}$$

2.2.4. Reynolds Number, Re

This number is defined as the ratio of inertia force to the viscous force. It is given as;

$$Re = \frac{\rho VL}{\mu}$$

This number signifies the relative predominance of the inertia to the viscous force occurring in the flow systems.

2.3. Problem Modelling

In this study, the fluid viscosity is taken as a linear function of temperature and can be illustrated as: $\mu = \mu_\infty [1 + \gamma(T - T_w)]$ where T is the temperature of the fluid and T_w is the temperature of the ambient fluid.

The non-dimensional variables used in transforming the

$$\frac{\partial u^*}{\partial t^*} + u^* \frac{\partial u^*}{\partial x^*} + v^* \frac{\partial u^*}{\partial y^*} = \frac{1}{\rho} \frac{\partial}{\partial y^*} \left(\mu \frac{\partial u^*}{\partial y^*} \right) + g\beta(T - T_\infty) \text{Sin} \left(\frac{x^*}{a} \right) - \frac{\delta_0\beta_0^2}{\rho} u^* \tag{9}$$

Substituting the variables in equation (6), equation (9) becomes;

$$\frac{Re a^2}{Gr^{\frac{1}{2}} U^2} \frac{\partial u}{\partial t} + u \frac{\partial u}{\partial x} + Gr^{\frac{1}{4}} v \frac{\partial u}{\partial y} = (1 + \gamma\theta) \frac{\partial^2 u}{\partial y^2} + \gamma \frac{\partial \theta}{\partial y} \frac{\partial u}{\partial y} + \theta \text{Sin} x - Mu \tag{10}$$

Equation (4) is the general equation of energy in two-dimensional form reduces as follows through mathematical formulation;

$$\frac{\partial T^*}{\partial t^*} + u^* \frac{\partial T^*}{\partial x^*} + v^* \frac{\partial T^*}{\partial y^*} = \frac{K}{\rho C_p} \frac{\partial^2 T^*}{\partial y^{*2}} \tag{11}$$

Substituting variables in equation (6), this equation becomes;

$$\frac{Re a^2}{Gr^{\frac{1}{2}} U^2} \frac{\partial \theta}{\partial t} + u \frac{\partial \theta}{\partial x} + Gr^{\frac{1}{4}} v \frac{\partial \theta}{\partial y} = \frac{1}{Pr} \frac{\partial^2 \theta}{\partial y^2} \tag{12}$$

Initial conditions:

$$u = v = 0, \theta = 1 \text{ at } t = 0 \tag{13a}$$

Boundary conditions:

general equations (1), (3) and (4) into non-dimensional form are given as follows;

$$x = \frac{x^*}{a}, y = \frac{Gr^{\frac{1}{4}}}{a} y^*, u = \frac{\rho a}{\mu} Gr^{\frac{-1}{2}} u^*, v = \frac{\rho a}{\mu} Gr^{\frac{-1}{2}} v^*, \theta = \frac{T^* - T_\infty}{T_w - T_\infty}, \gamma = \frac{1}{\mu_f} \left(\frac{\partial \mu}{\partial T} \right)_f (T_w - T_\infty), r(x^*) = a \text{Sin} \left(\frac{x^*}{a} \right), t = \frac{a}{U} t^* \tag{6}$$

Through mathematical formulation, the general equation of conservation of mass reduces to:

$$\frac{\partial (ru^*)}{\partial x^*} + Gr^{\frac{1}{4}} \frac{\partial (rv^*)}{\partial y^*} = 0 \tag{7}$$

Equation (7) is a dimensional equation of conservation of mass. Substituting the variables in equation (6) we obtain the non-dimensionalized equation which is given as;

$$\frac{\partial (ru)}{\partial x} + Gr^{\frac{1}{4}} \frac{\partial (rv)}{\partial y} = 0 \tag{8}$$

The general equation (3) of motion reduces to;

$$u = v = 0, \theta = 1, y = 0 \text{ at any } t \tag{13b}$$

$$u \rightarrow 0, \theta \rightarrow 0 \text{ as } y \rightarrow \infty \tag{13c}$$

2.4. Method of Solution

The Direct Numerical Scheme (DNS) method is applied in order to solve equations (8), (11) and (12). The following set of transformations is introduced in order to make it easier for these equations to be solved using this method:

$$X = x, Y = y, U = \frac{u}{x}, V = \frac{v}{y}, t = T(\text{time}). \text{ Therefore, } u = UX = UX \text{ and } v = Vy = VY. \tag{14}$$

$r(\hat{x})$ is the radial distance from the Centre of the sphere in consideration and is given as $r(x) = \text{Sin} X$ after non-

dimensionalization.

Substituting transformations (14) in equations (8), (11) and (12) and simplifying, these equations become;

$$\frac{\partial U}{\partial X} + \left[1 + X \frac{\cos X}{\sin X} \right] U + Gr^{\frac{1}{4}} V + Gr^{\frac{1}{4}} Y \frac{\partial V}{\partial Y} = 0 \quad (15)$$

$$\frac{Re a^2}{Gr^{\frac{1}{4}} U^2} \frac{\partial U}{\partial T} + UX \frac{\partial U}{\partial X} + U^2 + Gr^{\frac{1}{4}} VY \frac{\partial U}{\partial Y} = (1 + \gamma \theta) \frac{\partial^2 U}{\partial Y^2} + \gamma \frac{\partial \theta}{\partial Y} \frac{\partial U}{\partial Y} + \theta \frac{\sin X}{X} - MU \quad (16)$$

$$\frac{Re a^2}{Gr^{\frac{1}{4}} U^2} \frac{\partial \theta}{\partial T} + UX \frac{\partial \theta}{\partial X} + Gr^{\frac{1}{4}} VY \frac{\partial \theta}{\partial Y} = \frac{1}{Pr} \frac{\partial^2 \theta}{\partial Y^2} \quad (17)$$

conditions as used in the previous section can be given as:

Initial conditions;

$$U = V = 0, \theta = 1, T = 0 \text{ for all } X \text{ and } Y \quad (20a)$$

Boundary conditions;

$$U = V = 0, \theta = 1 \text{ at } X = 0 \text{ any } Y \text{ for all } T \quad (20b)$$

$$U = V = 0, \theta = 1 \text{ at } Y = 0, X > 0 \text{ for all } T \quad (20c)$$

$$U \rightarrow 0, \theta \rightarrow 0, \text{ as } Y \rightarrow \infty, X > 0 \text{ for all } T \quad (20d)$$

In order to determine the physical quantities, namely the shearing stress and the rate of heat transfer, the following dimensionless relations are used in this study;

$$\frac{C_f Gr^{\frac{1}{4}}}{2(1 + \gamma)} = X \left(\frac{\partial U}{\partial Y} \right)_{Y=0} \quad (18)$$

$$Nu Gr^{\frac{-1}{4}} = - \left(\frac{\partial \theta}{\partial Y} \right)_{Y=0} \quad (19)$$

Equations (17),(18),(19),(20) and (21) can be written in terms of finite differences as shown below;

Using transformations (14), the initial and boundary

$$X_i \left[\frac{U_{i+1,j}^k - U_{i-1,j}^k}{2(\Delta X)} \right] + \left[1 + X_i \frac{\cos X_i}{\sin X_i} \right] U_{i,j}^k + Gr^{\frac{1}{4}} \left[\frac{V_{i,j+1}^k + V_{i,j-1}^k}{2} \right] + Gr^{\frac{1}{4}} Y_j \left[\frac{V_{i,j+1}^k + V_{i,j-1}^k}{2(\Delta Y)} \right] = 0 \quad (21)$$

Making $U_{i,j}^k$ the subject of the formula in equation (21) gives;

$$U_{i,j}^k = - \left[X_i \left[\frac{U_{i+1,j}^k - U_{i-1,j}^k}{2(\Delta X)} \right] + Gr^{\frac{1}{4}} \left[\frac{V_{i,j+1}^k + V_{i,j-1}^k}{2} \right] + Gr^{\frac{1}{4}} Y_j \left[\frac{V_{i,j+1}^k + V_{i,j-1}^k}{2(\Delta Y)} \right] \right] \div \left[1 + X_i \frac{\cos X_i}{\sin X_i} \right] \quad (22)$$

Writing equation (16) in finite difference form and making $U_{i,j}^k$ the subject of the formulae, we obtain;

$$\begin{aligned} & \frac{Re a^2}{Gr^{\frac{1}{4}} U^2} \left[\frac{U_{i,j}^{k+1} - U_{i,j}^k}{2(\Delta T)} \right] + X_i \left[\frac{U_{i+1,j}^k + U_{i-1,j}^k}{2} \right] \left[\frac{U_{i+1,j}^k - U_{i-1,j}^k}{2(\Delta X)} \right] + \left[\frac{U_{i+1,j}^k + U_{i-1,j}^k}{2} \right]^2 + \\ & Gr^{\frac{1}{4}} Y_j \left[\frac{V_{i,j+1}^k + V_{i,j-1}^k}{2} \right] \left[\frac{U_{i,j+1}^k - U_{i,j-1}^k}{2(\Delta Y)} \right] = [1 + \gamma \theta_{i,j}^k] \left[\frac{U_{i,j+1}^k - 2U_{i,j}^k + U_{i,j-1}^k}{(\Delta Y)^2} \right] + \\ & \gamma \left[\frac{\theta_{i,j+1}^k - \theta_{i,j-1}^k}{2(\Delta Y)} \right] \left[\frac{U_{i,j+1}^k - U_{i,j-1}^k}{2(\Delta Y)} \right] + \theta_{i,j}^k \frac{\sin X_i}{X_i} - MU_{i,j}^k \end{aligned} \quad (23)$$

Therefore, making $U_{i,j}^{k+1}$ the subject of the formula, the equation can be written as:

$$\begin{aligned} U_{i,j}^{k+1} = & \frac{Re a^2}{Gr^{\frac{1}{4}} U^2} \left[\frac{1}{2(\Delta T)} \right] U_{i,j}^k + \left[1 + \gamma \theta_{i,j}^k \right] \left[\frac{U_{i,j+1}^k - 2U_{i,j}^k + U_{i,j-1}^k}{(\Delta Y)^2} \right] + \gamma \left[\frac{\theta_{i,j+1}^k - \theta_{i,j-1}^k}{2(\Delta Y)} \right] \left[\frac{U_{i,j+1}^k - U_{i,j-1}^k}{2(\Delta Y)} \right] \\ & + \left[\theta_{i,j}^k \frac{\sin X_i}{X_i} - MU_{i,j}^k \right] - \left[X_i \left[\frac{U_{i+1,j}^k + U_{i-1,j}^k}{2} \right] \left[\frac{U_{i+1,j}^k - U_{i-1,j}^k}{2(\Delta X)} \right] + \left[\frac{U_{i+1,j}^k + U_{i-1,j}^k}{2} \right]^2 \right] \\ & - \left[Gr^{\frac{1}{4}} Y_j \left[\frac{V_{i,j+1}^k + V_{i,j-1}^k}{2} \right] \left[\frac{U_{i,j+1}^k - U_{i,j-1}^k}{2(\Delta Y)} \right] \right] \div \left[\frac{Re a^2}{Gr^{\frac{1}{4}} U^2} \left[\frac{1}{2(\Delta T)} \right] \right] \end{aligned} \quad (24)$$

Writing equation (17) in terms of finite differences, it results to;

$$\frac{Re a^2}{Gr^{\frac{1}{2}} U^2} \left[\frac{\theta_{i,j}^{k+1} - \theta_{i,j}^k}{2(\Delta T)} \right] + X_i \left[\frac{U_{i+1,j}^k + U_{i-1,j}^k}{2} \right] \left[\frac{\theta_{i+1,j}^k - \theta_{i-1,j}^k}{2(\Delta X)} \right] + Gr^{\frac{1}{4}} Y_j \left[\frac{V_{i,j+1}^k + V_{i,j-1}^k}{2} \right] \left[\frac{\theta_{i,j+1}^k - \theta_{i,j-1}^k}{2(\Delta Y)} \right] = \frac{1}{Pr} \left[\frac{\theta_{i+1,j}^k - 2\theta_{i,j}^k + \theta_{i-1,j}^k}{(\Delta Y)^2} \right] \tag{25}$$

Making $\theta_{i,j}^{k+1}$ the subject of the formula, this equation can be written as;

$$\theta_{i,j}^{k+1} = \frac{Re a^2}{Gr^{\frac{1}{2}} U^2} \left[\frac{1}{2(\Delta T)} \right] \theta_{i,j}^k + \frac{1}{Pr} \left[\frac{\theta_{i+1,j}^k - 2\theta_{i,j}^k + \theta_{i-1,j}^k}{(\Delta Y)^2} \right] - \left[X_i \left[\frac{U_{i+1,j}^k + U_{i-1,j}^k}{2} \right] \left[\frac{\theta_{i+1,j}^k - \theta_{i-1,j}^k}{2(\Delta X)} \right] \right] - \left[Gr^{\frac{1}{4}} Y_j \left[\frac{V_{i,j+1}^k + V_{i,j-1}^k}{2} \right] \left[\frac{\theta_{i,j+1}^k - \theta_{i,j-1}^k}{2(\Delta Y)} \right] \right] \div \left[\frac{Re a^2}{Gr^{\frac{1}{2}} U^2} \left[\frac{1}{2(\Delta T)} \right] \right] \tag{26}$$

The physical quantities to be obtained are the shearing stress (rate of skin friction) and the rate of heat transfer. The finite difference equations used to obtain these results are;

$$\frac{C_f Gr^{\frac{1}{4}}}{2(1+\gamma)} = X_i \left(\frac{U_{i,j+1}^k - U_{i,j-1}^k}{2(\Delta Y)} \right)_{Y=0} \tag{27}$$

$$Nu Gr^{\frac{-1}{4}} = - \left(\frac{\theta_{i,j+1}^k - \theta_{i,j-1}^k}{2(\Delta Y)} \right)_{Y=0} \tag{28}$$

Equations (22), (24) (26), (27) and (28) are the final equations which are implemented in MATLAB in order to obtain the required results.

3. Results and Discussion

In this study, an investigation of the effects of variable viscosity on unsteady natural convection hydromagnetic flow past an isothermal sphere has been carried out. Viscosity is taken as a linear function of Temperature, therefore, viscosity varies directly proportional to temperature in this study. The numerical solutions start from the lower stagnation point $x = 0$, round the sphere to the upper stagnation point where $x = \pi$. The Reynolds number is taken as; Re (=3, 4, 5), Grashof number, Gr (=50, 65, 85, 100), Magnetic parameter, M (=0, 0.25, 0.5, 1) and Viscous variation parameter, γ (=0, 0.25, 0.5, 1).

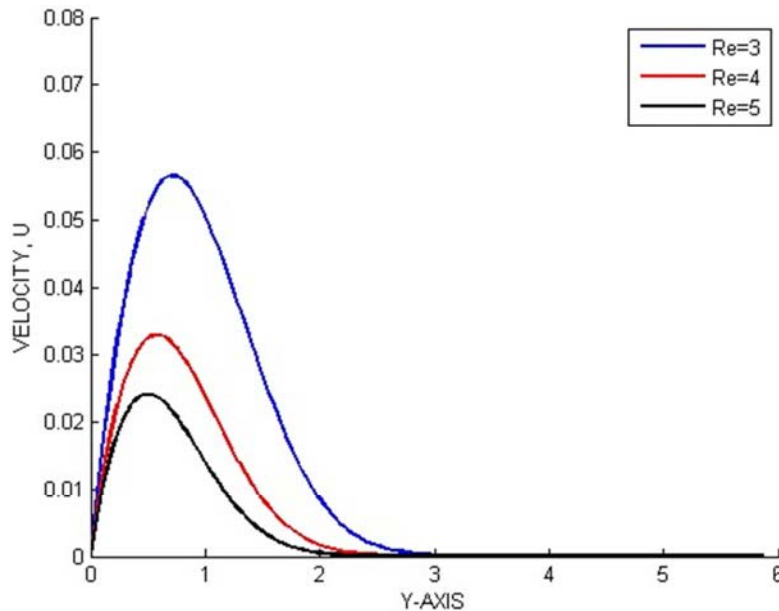


Figure 2. Primary velocity (U) against y-axis varying Reynolds number.

Figure 2 above represents the primary velocity (U) against the Y-axis varying Reynolds number. The Magnetic parameter is taken as M=0.5, Gr=85, γ =0.5 and Re (=3, 4,

5). It is observed that velocity profiles decreases with increase in Reynolds number and increases with decrease in Reynolds number. In this study, Re is considered as an

inverse function and thus increase in Re leads to increase in the viscosity of the fluid and decrease in Re leads to decrease in the viscosity. Increasing viscosity leads to an increase in the viscous force that opposes the motion of the fluid and decrease in viscosity leads to a decrease in the viscous force. Therefore, in this case, it can be concluded that increase in Reynolds number leads to an increase in the viscosity of the fluid and thus the decrease in the velocity of the fluid which leads to decrease in the velocity profiles.

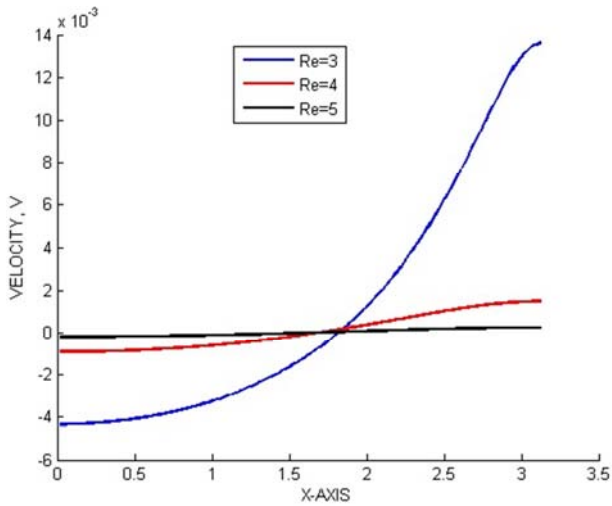


Figure 3. Secondary velocity (V) against X -axis varying Reynolds number.

Figure 3 above represents secondary velocity against the x -axis varying Reynolds number where $M=0.5$, $Gr=85$, $\gamma=0.5$ and $Re (=3, 4, 5)$. It is observed that the velocity starts from a negative value and increase to a positive value. Increase in Reynolds number leads to an increase in the velocity profiles until there is no change in the velocity profile at point (0). There is an intersection of the velocity profiles as observed from the above figure. This is because there is a circular motion displayed by the fluid which leads to a vortex flow. This leads to a change in the pressure gradient of the flow and thus the secondary flow of the fluid at the floor of the sphere changes as shown in the diagram above with increase in the Reynolds number.

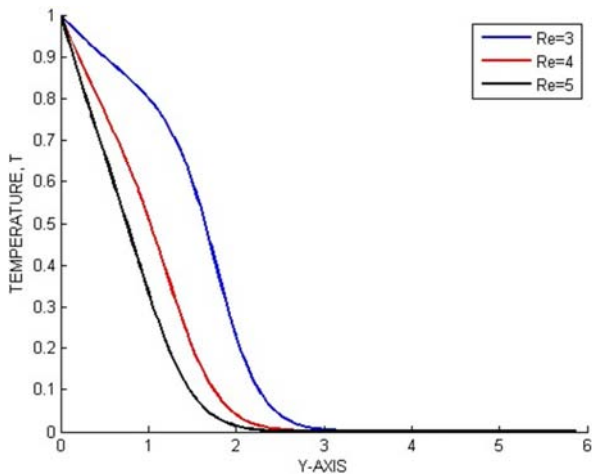


Figure 4. Temperature (T) against Y -axis varying Reynolds number.

From figure 4 above, $M=0.5$, $Gr=85$, $\gamma=0.5$ and $Re (=3, 4, 5)$ and it is observed that increase in Reynolds number leads to decrease in the temperature profiles and decrease in Re leads to increase in the temperature profiles. In this study, Re is considered as an inverse function and thus increase in Re leads to increase in the viscosity of the fluid and decrease in Re leads to decrease in the viscosity. Increasing viscosity leads to an increase in the viscous force that opposes the motion of the fluid and decrease in viscosity leads to a decrease in the viscous force. Therefore, in this case, it can be concluded that increase in Reynolds number leads to an increase in the viscosity of the fluid and thus the decrease in the temperature of the fluid which leads to decrease in the temperature profiles.

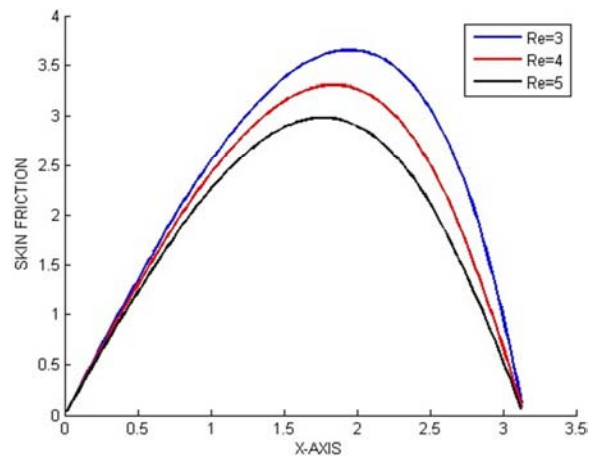


Figure 5. Skin friction against x -axis varying Reynolds number.

Figure 5 represents the skin friction against the X -axis varying Reynolds number while $M=0.5$, $Gr=85$ and $\gamma=0.5$. It is observed that the skin-friction profiles decreases with increase in Reynolds number and increases with decrease in Reynolds number. Increase in Re leads to increase in the viscosity of the fluid which leads to increase in the viscous force due to the inverse nature of Reynolds number in this study. Increased viscous force leads to a reduction in the velocity of the fluid and thus the reduction in the velocity gradient. Decrease in velocity gradient leads to a decrease in the skin friction in the fluid as portrayed in the profiles above.

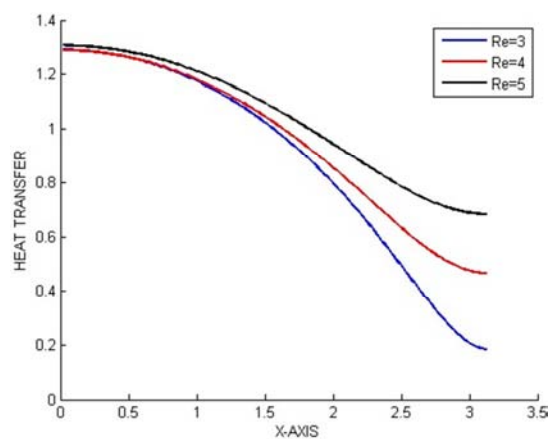


Figure 6. Heat transfer against x -axis varying Reynolds number.

Figure 6 above shows the Heat transfer against x-axis varying Reynolds number whereas $M=0.5$, $Gr=85$ and $\gamma=0.5$. It can be observed that increase in Reynolds number leads to an increase in the Heat transfer profiles and decrease in Reynolds number leads to a decrease in the heat transfer profiles. Increase in Re leads to increase in the viscosity of the fluid which leads to increase in the viscous force due to the inverse nature of Reynolds number in this study. Increased viscous force leads to a reduction in the temperature of the fluid and thus the reduction in the temperature gradient. Decrease in the temperature gradient of the fluid leads to an increase in the heat transfer of the fluid.

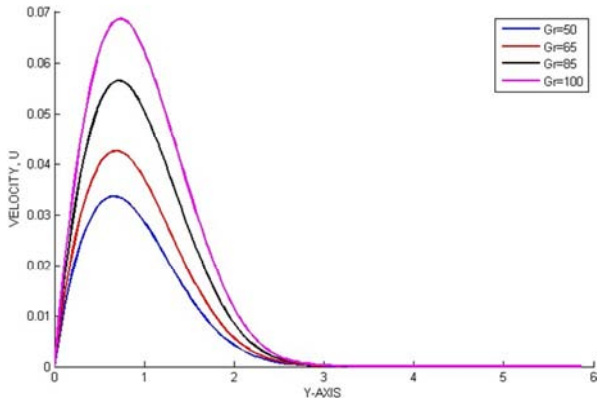


Figure 7. Primary velocity (U) against Y-axis varying Grashof number.

Figure 7 above represents the primary Velocity against Y-axis varying the Grashof number while $M=0.5$, $Re=4$ and $\gamma=0.5$. It is observed that increase in Grashof number leads to an increase in the velocity profiles and decrease in Grashof number leads to decrease in the velocity profiles. Increase in Grashof number leads to decrease in the viscosity of the fluid and decrease in Grashof number leads to an increase in the viscosity of the fluid. Increase in the viscosity of the fluid leads to an increase in the viscous force which leads to a decrease in the velocity of the fluid and decrease in the viscosity leads to decrease in the viscous force thus increase in the velocity of the fluid. Therefore, increase in Grashof number leads to a decrease in Viscosity which reduces the viscous force and thus an increase in the velocity of the fluid as shown in the figure 7 above.

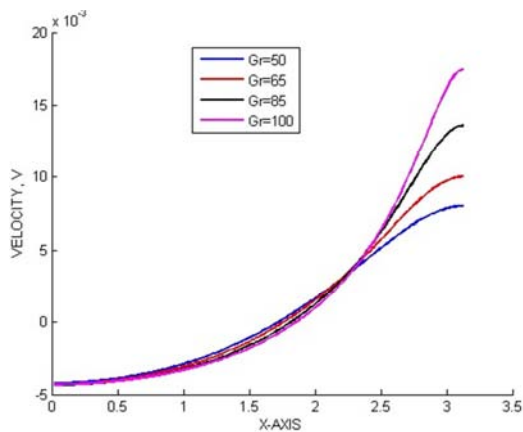


Figure 8. Secondary velocity (V) against x-axis varying Grashof number.

From figure 8 above, it is observed that there is a slight decrease in the velocity profiles when the Grashof number is increased. The profiles intersect at a point and begin to increase after the same point in an inverse behavior. This is because of the circular motion displayed by the fluid which leads to a vortex flow which causes a change in pressure gradient of the flow and thus the secondary flow of the fluid across the floor of the sphere.

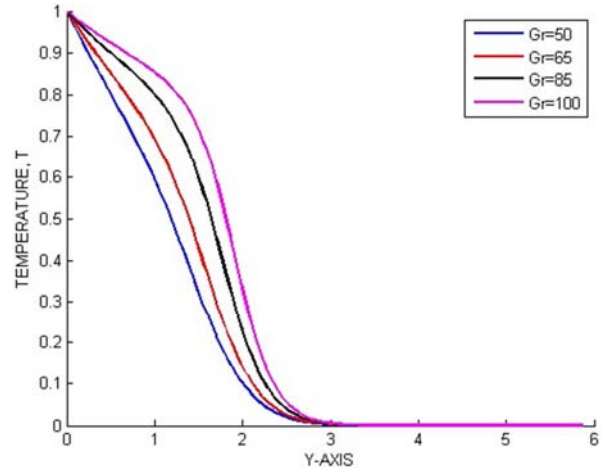


Figure 9. Temperature (T) against Y-axis varying Grashof number.

Figure 9 above shows the temperature (T) against the Y-axis varying Grashof number while $M=0.5$, $Re=4$ and $\gamma=0.5$. It can be observed that increase in Grashof number leads to an increase in the temperature profiles and decrease in Grashof number leads to a decrease in Grashof number. Increase in Grashof number leads to decrease in the viscosity of the fluid and decrease in Grashof number leads to an increase in the viscosity of the fluid. Increase in the viscosity of the fluid leads to an increase in the viscous force which leads to a decrease in the temperature of the fluid and decrease in the viscosity leads to decrease in the viscous force thus increase in the temperature of the fluid. Therefore, increase in Grashof number leads to a decrease in Viscosity which reduces the viscous force and thus an increase in the temperature of the fluid and thus the increase in the temperature profiles.

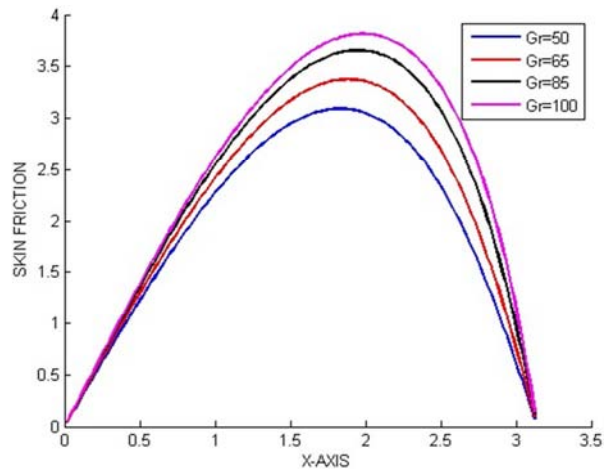


Figure 10. Skin Friction against X-axis varying Grashof number.

Figure 10 above shows the profiles of skin friction against x-axis varying Grashof number while $M=0.5$, $Re=4$ and $\gamma =0.5$. It is observed that increase in Grashof number leads to an increase in the skin friction profiles and decrease in Grashof number leads to a decrease in skin friction. Increase in Grashof number leads to decrease in the viscosity of the fluid and decrease in Grashof number leads to an increase in the viscosity of the fluid. Increase in the viscosity of the fluid leads to an increase in the viscous force which leads to a decrease in

the velocity of the fluid and decrease in the viscosity leads to increase in the velocity of the fluid. Decrease in velocity leads to a decrease in the velocity gradient of the fluid and increase in the velocity leads to an increase in the velocity gradient of the fluid. Therefore, in this case, increase in Grashof number leads to an increase in the velocity gradient of the fluid which leads to an increase in the skin friction of the fluid.

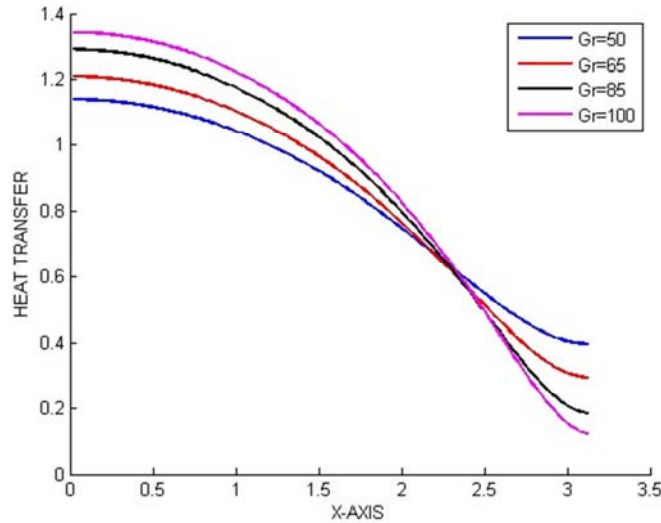


Figure 11. Heat transfer against x-axis varying Grashof number.

Figure 11 above shows the profiles of Heat transfer against x-axis varying Grashof number while $M=0.5$, $Re=4$ and $\gamma =0.5$. It is observed that increase in Grashof number leads to an increase in Heat transfer profiles and decrease in Grashof number leads to a decrease in the heat transfer. Increase in Grashof number leads to decrease in the viscosity of the fluid and decrease in Grashof number leads to an increase in the viscosity of the fluid. Increase in the viscosity of the fluid leads to an increase in the viscous force which leads to a decrease in the temperature of the fluid and decrease in the viscosity leads to decrease in the viscous force thus increase in the temperature of the fluid. Increase in temperature leads to an increase in temperature gradient of the fluid which leads to an increase in the heat transfer as shown in the figure above.

Figure 12 shows Primary velocity against Y-axis varying Magnetic parameter where M ($=0, 0.25, 0.5, 1.0$) whereas $Gr=85$, $Re=4$ and $\gamma =0.5$. It is observed that increase in Magnetic parameter leads to decrease in the velocity profiles and decrease in Magnetic parameter leads to an increase in the velocity profiles. Increase in Magnetic parameter leads to an increase in Lorentz force in the fluid which opposes the fluid flow and thus leading to a decrease in the velocity of the fluid thus the reduction in the velocity profiles shown above.

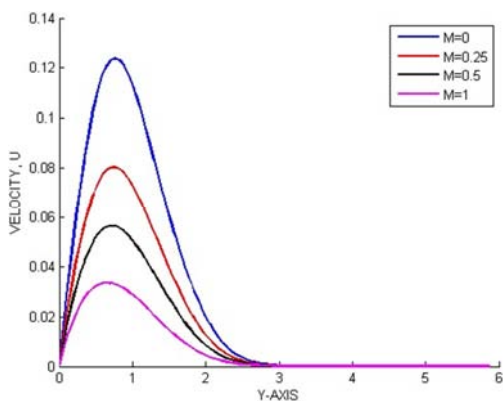


Figure 12. Primary velocity (U) against Y-axis varying Magnetic parameter M.

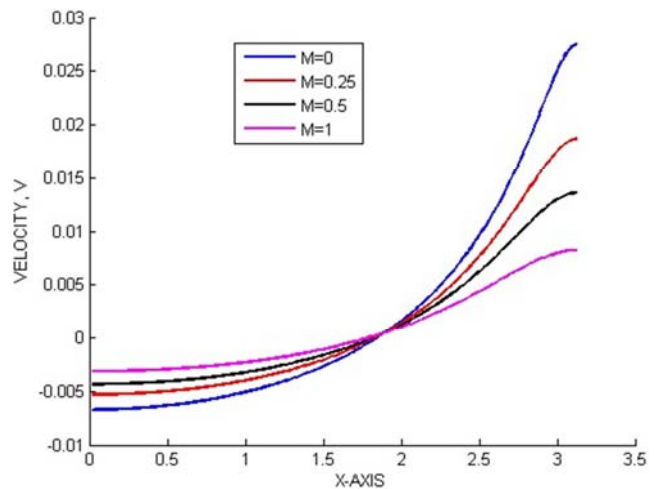


Figure 13. Secondary velocity (V) against x-axis varying Magnetic parameter (M).

Figure 13 above shows the Secondary velocity (V)

against x-axis varying magnetic parameter (M) whereas $Gr=85$, $Re=4$ and $\gamma=0.5$. Increase in Magnetic parameter leads to an increase in the velocity profiles and decrease in the magnetic parameter leads to a decrease in the velocity profiles. There is an intersection of the velocity profiles at a certain point and then the profiles starts to rise. This is because as the fluid passes below the sphere, there is a circular motion that is displayed by the fluid which leads to a vortex flow. This makes the surface of the fluid to have a characteristic depression toward the axis of the spinning fluid.

At any elevation with the fluid, the pressure is a little greater near the perimeter of the sphere where the fluid is a little deeper than near the center of the sphere. The fluid pressure is a little greater where the speed of the fluid is a little slower and the pressure is a little less where the speed is faster and therefore, this is consistent with the Bernoulli's principle. There is a pressure gradient from the perimeter of the sphere to towards the center which leads to a centripetal force which is necessary for the circular motion of each parcel of the fluid. This pressure gradient accounts for the secondary flow of the boundary layer of the fluid flowing across the floor of the fluid. Thus, the variation of the velocity profiles with the magnetic parameter as shown above.

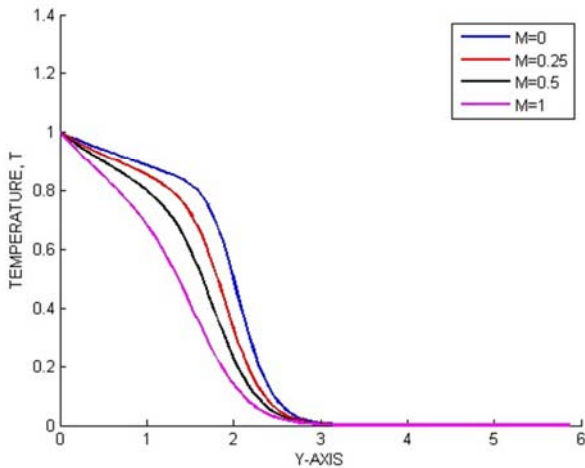


Figure 14. Temperature (T) against Y-axis varying Magnetic parameter.

Figure 14 represents temperature (T) against Y-axis varying Magnetic parameter (M) while $Gr=85$, $Re=4$ and $\gamma=0.5$. It is observed that increase in Magnetic parameter M leads to a decrease in the temperature profiles whereas decrease in magnetic parameter leads to an increase in the temperature profiles. Increase in the Magnetic parameter leads to an increase in the Lorentz force in the fluid which leads to a decrease in the temperature of the fluid and decrease magnetic parameter leads to a decrease in Lorentz force which leads to an increase in the Temperature of the fluid, thus the change in the temperature profiles.

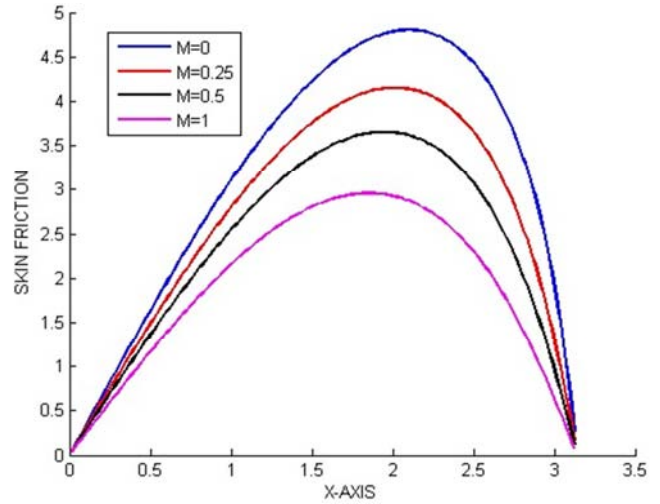


Figure 15. Skin friction against X-axis varying Magnetic parameter.

Figure 15 above represents Skin friction against x-axis varying Magnetic parameter while $Gr=85$, $Re=4$ and $\gamma=0.5$. It is observed that increase in the Magnetic parameter leads to decrease in the sin friction and decrease in the magnetic parameter leads to an increase in the skin friction of the fluid. This can be explained from the fact that increase in Magnetic parameter leads to increase in Lorentz force which opposes the motion of the fluid and this leads to a decrease in the velocity gradient which leads to decrease in the local skin friction coefficient and hence the reduction in the skin friction profiles.

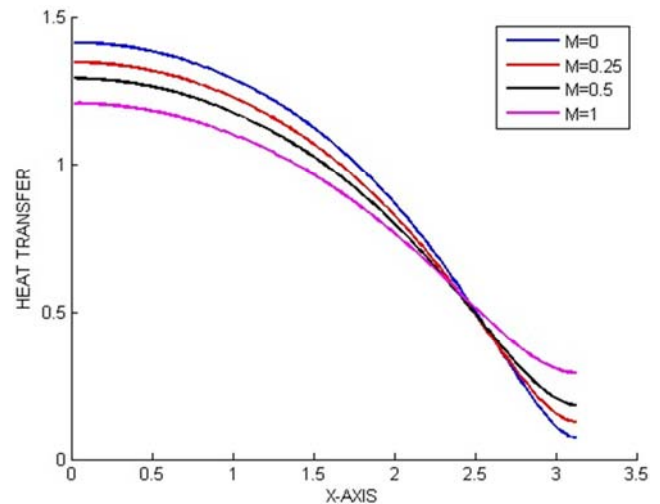


Figure 16. Heat Transfer against X-axis varying Magnetic parameter.

Figure 16 above shows Heat transfer against X-axis varying Magnetic parameter M while $Gr=85$, $Re=4$ and $\gamma=0.5$. It is observed that increase in Magnetic parameter leads to a decrease in the heat transfer and decrease in Magnetic parameter leads to an increase in the heat transfer. This is because increase in Magnetic parameter leads to an increase in Lorentz force which opposes the motion of the fluid and leads to a decrease in the temperature gradient and hence the decrease in the local Nusselt number. For increasing fluid temperature, the temperature difference between fluid and the

surface decreases and hence the corresponding rate of heat transfer decreases.

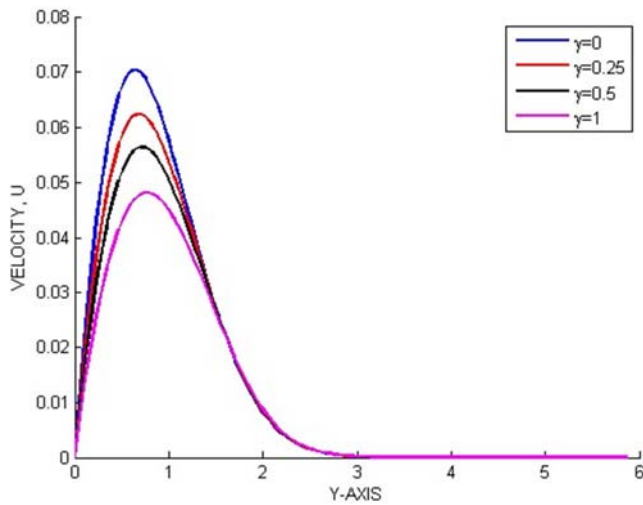


Figure 17. Velocity (U) against Y-axis varying the viscous variation parameter.

Figure 17 above shows the primary velocity (U) against Y-axis varying the viscous variation parameter γ while $Gr=85$, $Re=4$ and $M=0.5$. From the figure, it is observed that increase in γ leads to a decrease in the velocity (U) of the fluid and decrease in γ leads to an increase in the velocity of the fluid. For increasing values of γ , the viscosity of the fluid within the boundary layer increases which retards the fluid motion and as a result, the velocity (U) of the fluid decreases.

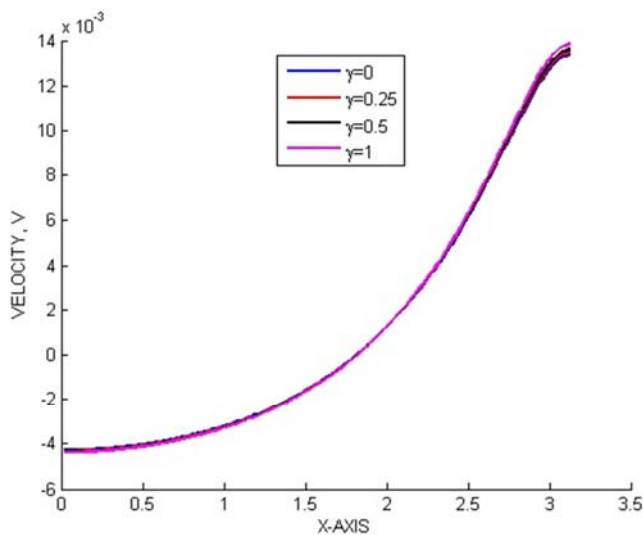


Figure 18. Velocity (V) against X-axis varying Viscous Variation Parameter.

Figure 18 above represents Secondary velocity (V) against X-axis varying the Viscous variation parameter (γ) while $Gr=85$, $Re=4$ and $M=0.5$. From the figure, it is observed that there is a slight change in the velocity profiles. This is because there is a slight effect of viscosity of the fluid on the secondary velocity of the fluid.

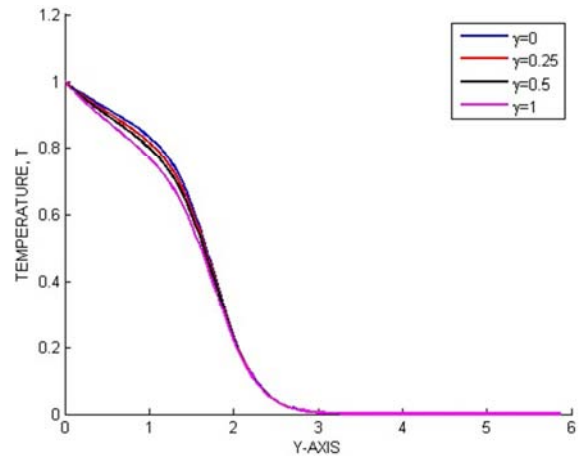


Figure 19. Temperature (T) against Y-axis varying Viscous Variation parameter.

Figure 19 above represents temperature (T) against Y-axis varying the viscous variation parameter while $Gr=85$, $Re=4$ and $M=0.5$. It is observed that increase in γ leads to a decrease in the temperature of the fluid and decrease in γ leads to an increase in the temperature of the fluid. This is because increase in γ leads to an increase in the viscosity of the fluid which leads to an increase in viscous force which opposes the motion of the fluid. This increase in the viscous force leads to a decrease in the temperature of the flow and the reduction rate of the temperature profiles. The change in the temperature profiles is very slight which shows the change in the viscous variation parameter has a slight effect on the temperature profiles.

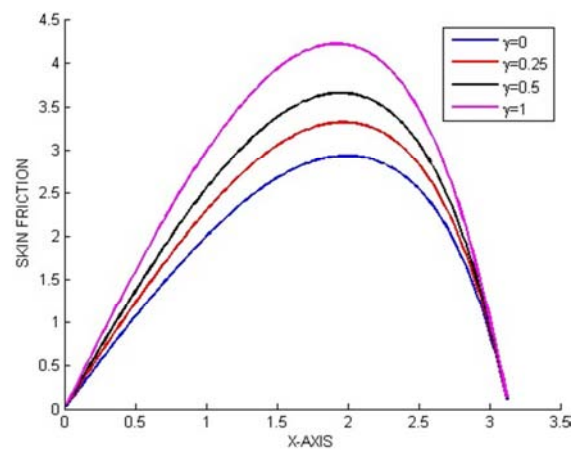


Figure 20. Skin friction against X-axis varying viscous variation parameter.

Figure 20 above shows Skin friction against X-axis varying the viscous variation parameter while $Gr=85$, $Re=4$ and $M=0.5$. From the figure above, it is observed that increase in viscous variation parameter leads to an increase in the skin friction of the fluid and a decrease in the skin friction leads to a decrease in the skin friction of the fluid. Skin friction varies directly proportional to the viscous variation parameter γ and therefore increase in γ leads to an increase in the skin friction and decrease in γ leads to a decrease in the skin friction. Thus, the change in the skin friction profiles

as shown above.

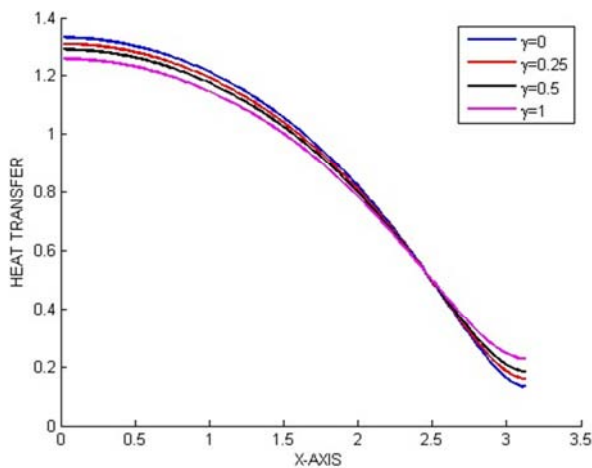


Figure 21. Heat transfer against X-axis varying viscous variation parameter.

Figure 21 above represents heat transfer against X-axis varying Viscous variation parameter while $Gr=85$, $Re=4$ and $M=0.5$. From the figure, it is observed that increase in γ leads to a decrease in the heat transfer profiles and decrease in γ leads to increase in the heat transfer profiles. It can be observed that increase in γ leads to a decrease in the temperature of the fluid and decrease in γ leads to an increase in the temperature of the fluid. This is because increase in γ leads to an increase in the viscosity of the fluid which leads to an increase in viscous force which opposes the motion of the fluid. Decrease in the temperature of the fluid with increase in the viscous variation parameter leads to a decrease in the temperature gradient which leads to a reduction in the rate of heat transfer which means that the Nusselt number decreases.

4. Conclusions

In this study, the effects of variable viscosity on unsteady natural convection hydromagnetic flow past an isothermal sphere has been carried out. The numerical results in this study have been obtained using the Direct Numerical Scheme (DNS). It can be concluded that;

- Increase in Reynolds number (Re) leads to an increase in the secondary velocity (V) and Heat transfer in the fluid but leads to a decrease in Primary velocity (U), Temperature (T) and Skin friction of the fluid.
- Increase in Grashof number leads to an increase in Primary velocity (U), Temperature, Skin friction and Heat transfer in the fluid but leads to a decrease in Secondary velocity (V).
- Increase in Magnetic parameter (M) leads to an increase in Secondary velocity (V) but leads to a decrease in primary velocity (U), Temperature, (T), Skin Friction and Heat transfer.
- Increase in the Viscous variation parameter (γ) leads to an increase in skin friction, a slight change in secondary velocity (V) but leads to a decrease in primary velocity

(U), Temperature and Heat transfer in the fluid.

Acknowledgement

I would like to thank my friend Steve Kamau for his support in the course of this work and Pan African University Institute for Basic Sciences, Technology and Innovation for the Scholarship awarded.

Nomenclature

a	Radius of the sphere, m
C_p	Specific heat at constant pressure, J/deg kg
C_f	Skin friction coefficient
f	Dimensionless stream function
g	Acceleration due to gravity, g
Gr	Grashof number
K	Thermal conductivity of the fluid, W/mK
Mu	MHD parameter
Nu	Nusselt number
Pr	Prandtl number
q_w	Heat flux at the surface, W/m ²
T	Temperature of the fluid, K
T_∞	Temperature of the ambient fluid, K
T_w	Temperature at the surface, K
u, v	Dimensionless velocity component
x, y	Axis direction
β	Volumetric coefficient of thermal expansion, (C ^o) ⁻¹
τ_w	Shearing stress, N/m ²
ρ	Density of the fluid, Kg/m ³
μ	Viscosity of the fluid, Ns/m ²
θ	Dimensionless temperature function
β_0	Strength of magnetic field, A/m
δ_0	Electric conduction, S/m
V	Fluid velocity in the x, y direction, m ³ /s
$\bar{\nabla}$ Gradient operator	$\bar{i} \frac{\partial}{\partial x} + \bar{j} \frac{\partial}{\partial y} + \bar{k} \frac{\partial}{\partial z}$
\bar{F}	Body forces vector in x and y directions, N
h_m	Magnetic field intensity, T
C_{fx}	Local skin Friction coefficient
Q	Heat Generation Parameter
$r(\hat{x})$	Radial distance from the symmetrical axis to the surface of the sphere, m
o	The Centre of the sphere

References

- [1] Molla M. M, Hossain A., Gorla R. S. R. (2005). Natural convection flow from an isothermal horizontal circular cylinder with temperature dependent viscosity. *Heat and mass transfer journal*. 41 (7): 594-598.

- [2] Selivanov N. V. and Kuz'min S. I. (2009). Numerical Simulation of Forced Flow in Boundary Layer and of Heat Transfer by Non-Newtonian Fluid in View of the Temperature Dependence of Viscosity. *Heat and Mass Transfer and Physical Gasdynamics*. 47 (6): 886-891.
- [3] Rahman M. M., Rahman M. A., Samad M., Alam S. (2009). Heat Transfer in Micropolar Fluid along a Non-Linear Stretching Sheet with Temperature Dependent Viscosity and Variable Surface Temperature. *International Journal of Thermophysics*. 30 (5): 1649-1670.
- [4] Gomathi P. and Kwang-Yong K. (2010). Numerical study on a vertical plate with variable viscosity and thermal conductivity. *Archive of Applied Mechanics*. 80 (7): 711-725.
- [5] Miyauchi A., Kameyama M., Ichikawa H. (2014). Linear stability analysis on the influences of the spatial variations in thermal conductivity and expansivity on the flow patterns of thermal convection with strongly temperature-dependent viscosity. *Journal of Earth Science*. 25 (1): 126-139.
- [6] Umavathi J. C. (2015). Combined Effect of Variable Viscosity and Variable Thermal Conductivity on Double Diffusive Convection Flow of a Permeable Fluid in a Vertical Channel. *Transport in Porous Media*. 108 (3).
- [7] Umavathi J. C. and Shekar M. (2015). Combined effect of variable viscosity and thermal conductivity on free convection flow of a viscous fluid in a vertical channel using DTM. *Meccanica*. pp 1-16.
- [8] Beg O. A., Zueco J., Ghosh S. K., Heidari A. (2011). Unsteady Magnetohydrodynamic Heat Transfer in a Semi-Infinite Porous Medium with Thermal Radiation Flux: Analytical and Numerical Study. *Advances in Numerical Analysis*: 2011 (304124), 17 pages.
- [9] Deka R. K. and Neog B. C (2009). Unsteady natural convection flow past an accelerated vertical plate in a thermally stratified fluid. *Theoret. Mech*. 36 (4): 261-274.
- [10] Mina B. A, Magda M. K, Mohammad L. M (2004). Similarity solutions for unsteady free-convection flow from a continuous moving vertical surface. *Journal of Computational and Applied Mathematics*. 11 – 24: 164–165.
- [11] Ramesh G. K., Mahesha, Gireesha B. J., Bagewadi C. S. (2011). Unsteady flow of a conducting dusty fluid between two circular cylinders. *Acta Math. Univ. Comenianae*. 80 (2): 171–184.
- [12] Mebine P. and Adigio E. M (2009). Unsteady Free Convection Flow with Thermal Radiation Past a Vertical Porous Plate with Newtonian Heating. *Turk J Phys*. 33: 109 – 119.
- [13] Deepa G. and Murali G. (2014). Effects of viscous dissipation on unsteady MHD free convective flow with thermophoresis past a radiate inclined permeable plate. *Iranian Journal of Science & Technology*. 38 (3): 379-388.
- [14] Sugunamma V. and Sandeep N. (2013). Effect of inclined magnetic field on unsteady free convection flow of a dusty viscous fluid between two infinite flat plates filled by a porous medium. *International Journal of Applied Mathematics and Modeling*. 1 (1): 16-33.